

Dalitz plot analysis of $D \rightarrow K \pi \pi$ decays

J. C. Anjos,^γ J. A. Appel,^ξ A. Bean,^α S. B. Bracker,^λ T. E. Browder,^{α,(a)} L. M. Cremaldi,^η
 G. M. Danner,^ι J. Duboscq,^{α,(b)} J. R. Elliott,^{ε,(c)} C. O. Escobar,^κ M. C. Gibney,^{ε,(d)} A. S. Gordon,^{ι,(e)} G. F. Hartner,^λ
 P. E. Karchin,^μ B. R. Kumar,^λ M. J. Losty,^θ G. J. Luste,^λ P. M. Mantsch,^ξ J. F. Martin,^λ S. McHugh,^α
 S. R. Menary,^{λ,(f)} R. J. Morrison,^α T. Nash,^ξ P. Ong,^λ J. Pinfold,^β G. Punkar,^{α,(g)} M. V. Purohit,^ι
 J. R. Raab,^{α,(h)} W. R. Ross,^μ A. F. S. Santoro,^γ A. L. Shoup,^{δ,(i)} J. S. Sidhu,^{β,(j)} K. Sliwa,^{ξ,(k)} M. D. Sokoloff,^δ
 M. H. G. Souza,^γ M. E. Streetman,^ξ A. B. Stundžia,^λ W. D. Volkmoth,^ι and M. S. Witherell^α

^αUniversity of California, Santa Barbara, California 93106

^βCarleton University, Ottawa, Ontario, Canada K1S 5B6

^γCentro Brasileiro de Pesquisas Físicas, Rio de Janeiro, Brazil

^δUniversity of Cincinnati, Cincinnati, Ohio 45221

^εUniversity of Colorado, Boulder, Colorado 80309

^ξFermi National Accelerator Laboratory, Batavia, Illinois 60510

^ηUniversity of Mississippi, University, Mississippi 38677

^θNational Research Council, Ottawa, Ontario, Canada K1A 0R6

^ιPrinceton University, Princeton, New Jersey 08544

^κUniversidade de São Paulo, São Paulo, Brazil

^λUniversity of Toronto, Toronto, Ontario, Canada M5S 1A7

^μYale University, New Haven, Connecticut 06511

(Received 2 December 1992)

Decays of the D^0 meson to $K^-\pi^+\pi^0$ and $\bar{K}^0\pi^+\pi^-$ and of the D^+ to $K^-\pi^+\pi^+$ have been analyzed for resonant substructure. We present results on the amplitudes and phases of each decay mode and compare the results with other measurements. We confirm the highly nonresonant nature of the D^+ to $K^-\pi^+\pi^+$ decays. There is general agreement with theoretical models for the branching ratios measured.

PACS number(s): 13.25.+m, 14.40.Ev, 14.40.Jz

I. INTRODUCTION

Hadronic decays of charmed particles have been a subject of much study in the past few years as new information from experiments has become available. Theorists have attempted to understand these data and have made predictions concerning hadronic decays [1,2]. Since the charm quark is not very heavy, charm hadrons decay mainly into two, three, and four particles. Here we examine three-body decays of the D^0 meson to $K^-\pi^+\pi^0$ and $\bar{K}^0\pi^+\pi^-$ and of the D^+ to $K^-\pi^+\pi^+$ to determine the fractions into two-body modes and the relative phases of the decay amplitudes. In this paper we implicitly include decays of antiparticles.

The data sample comes from the fixed-target photoproduction experiment E691 done at Fermilab during 1985 and described elsewhere [3]. The experiment recorded 100×10^6 events from which approximately 10,000 charm particle decays were reconstructed. We first describe the reconstruction and analysis common to all three modes and then describe the event selection specific to individual modes.

II. EVENT SELECTION

Events were selected by requiring that the D meson decay tracks satisfy a vertex hypothesis with a χ^2 per degrees of freedom (χ^2/N_{DF}) less than 3.5, that the reconstructed candidate D point back to within $80 \mu\text{m}$ of the primary vertex in the transverse plane, and that the primary vertex itself have a $\chi^2/N_{DF} < 6$. We further required that the separation of the primary and secondary vertices along the beam direction divided by the error on this quantity be larger than 6. In all three decay modes we required that the charged tracks go through at least one of our two analysis magnets and that each track have a particle identification probability based on Čerenkov information of at least 50%.

In the case of the $D^+ \rightarrow K^-\pi^+\pi^+$ decays, we required that there be no other tracks within $100 \mu\text{m}$ of the secondary vertex in the transverse direction. A signal of 4149 ± 79 events results (Fig. 1). In order to minimize backgrounds in both the D^0 decay modes, we select only

(a)Now at Cornell University, Ithaca, NY.

(b)Now at CERN, Geneva, Switzerland.

(c)Now at Electro Magnetic Applications, Inc., Denver, CO.

(d)Now at Nichols Research, Colorado Springs, CO.

(e)Now at Harvard University, Cambridge, MA.

(f)Now at the Univ. of California, Santa Barbara, CA.

(g)Now at SLAC, Stanford, CA.

(h)Now at Mainz University, Mainz, Germany.

(i)Now at the Univ. of California, Irvine, CA.

(j)Deceased.

(k)Now at Tufts University, Medford, MA.

those D^0 candidates which are products of D^{*+} decays. The pion from the D^{*+} decay was required to satisfy the same requirements as are the other charged tracks. In the $D^0 \rightarrow \bar{K}^0 \pi^+ \pi^-$ mode the Q value of the candidate D^{*+} decays was allowed to be within ± 1.5 MeV of the expected value and in the $D^0 \rightarrow K^- \pi^+ \pi^0$ mode to be within ± 2.5 MeV of the expected value. The K_S^0 decay tracks are required to go through both magnets, have a product particle identification probability greater than 5%, and a distance of closest approach of less than 5 mm (and $100 \mu\text{m}$ for the small fraction of K_S^0 that decay before the precision silicon vertex detector). The K_S^0 decay

volume was restricted to end upstream of the first magnet. The reconstructed K_S^0 mass was required to lie between 480 and 514 MeV/c^2 . In the $K^- \pi^+ \pi^0$ mode the π^0 particles were required to have at least 8 GeV in energy and lie outside the ‘‘pair plane,’’ a $\pm 3\text{-cm}$ band in our electromagnetic calorimeter where the entire background of e^+e^- pairs from low-energy bremsstrahlung photons appears. The reconstructed π^0 mass has a width of approximately 10 MeV, and a mass plot is shown in Ref. [4]. The signals for the $D^0 \rightarrow \bar{K}^0 \pi^+ \pi^-$ mode (174 ± 20 events) and for the $D^0 \rightarrow K^- \pi^+ \pi^0$ mode (317 ± 20 events) are shown in Fig. 1.

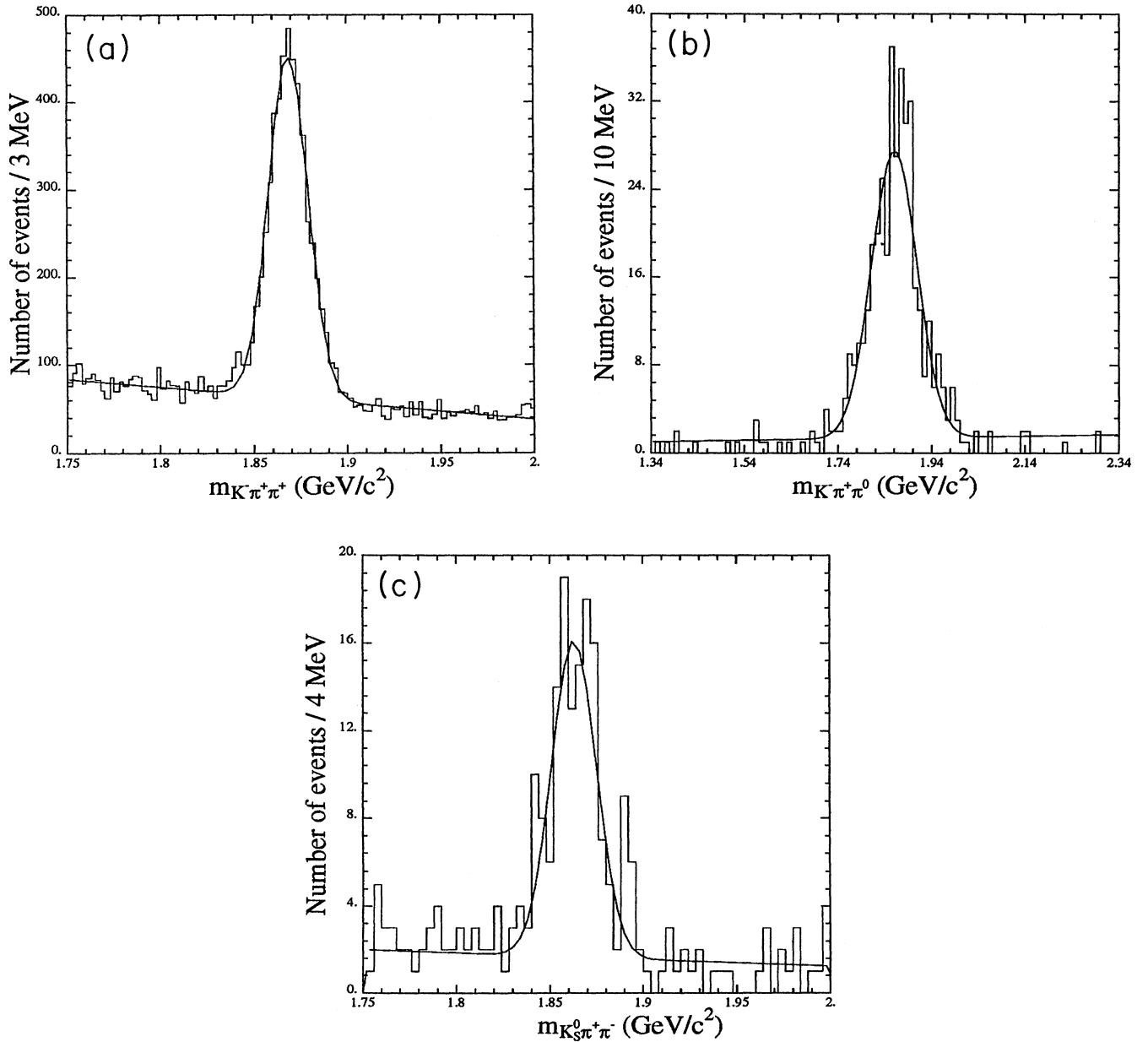


FIG. 1. Mass plots for (a) the $D^+ \rightarrow K^- \pi^+ \pi^+$ mode, (b) the $D^0 \rightarrow K^- \pi^+ \pi^0$ mode, and (c) the $D^0 \rightarrow \bar{K}_S^0 \pi^+ \pi^-$ mode.

III. ANALYSIS

Our technique for creating and fitting Dalitz plots is described here using the high-statistics mode $D^+ \rightarrow K^- \pi^+ \pi^+$ as an illustration. The same technique was used in all three modes. For the displayed D^+ Dalitz plot, we randomly order the two identical pions; the fitting functions are symmetrized, and so it does not affect the results. The Dalitz plots for the region containing the signal and for events in the background region are

shown in Fig. 2. Events are constrained to lie within the Dalitz-plot boundary by forcing the D^+ candidate mass [5] to $1.8693 \text{ GeV}/c^2$ and the D^0 candidate mass to [5] $1.8645 \text{ GeV}/c^2$ by scaling the momenta of the decay particles. These constraints reduce the smearing of events within the Dalitz plot. In the $D^+ \rightarrow K^- \pi^+ \pi^+$ and $D^0 \rightarrow \bar{K}^0 \pi^+ \pi^-$ modes the observed decay particles are all charged and hence the smearing was small. The three decay momenta were therefore scaled by the same factor.

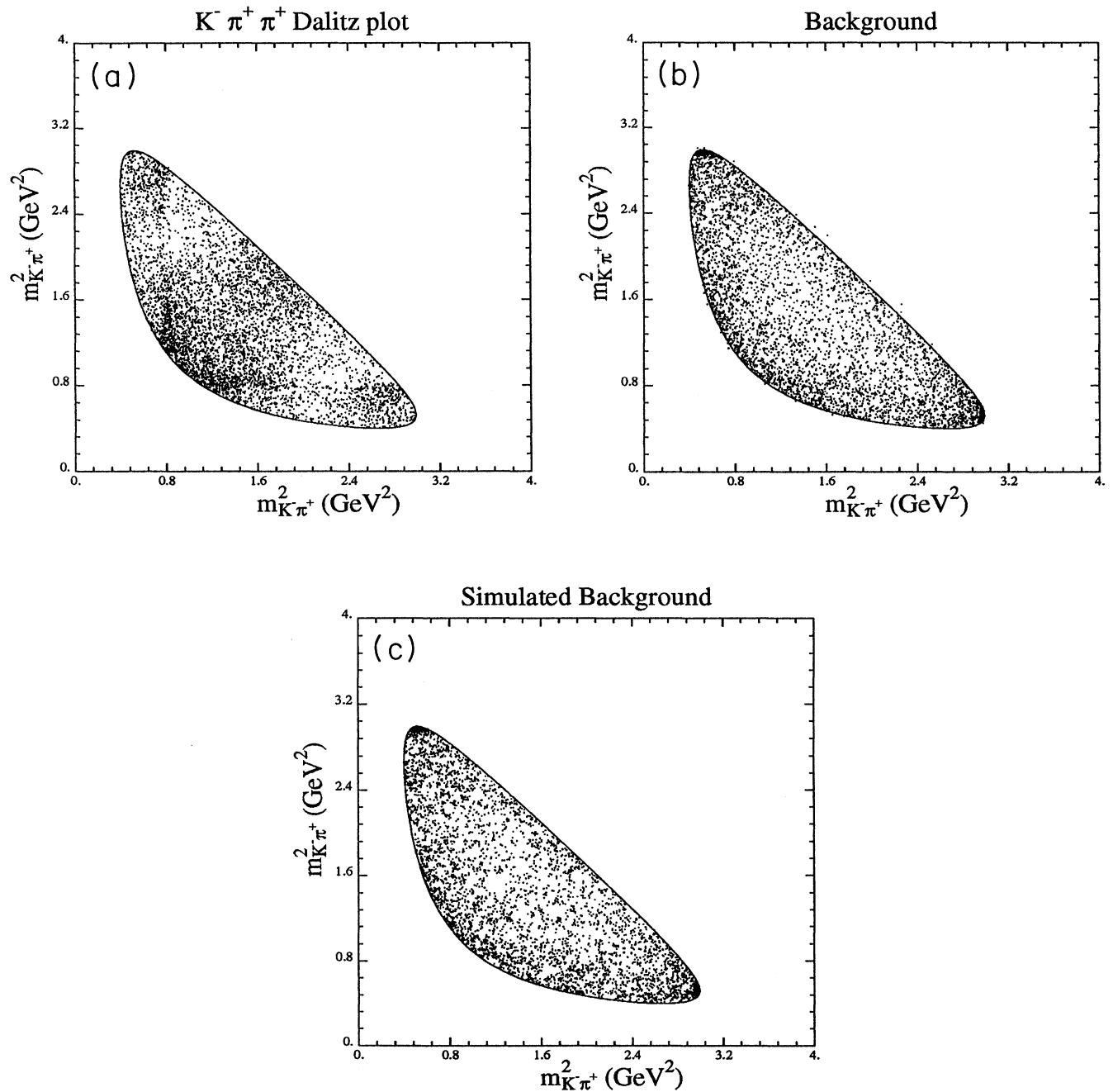


FIG. 2. Dalitz plots for (a) the $D^+ \rightarrow K^- \pi^+ \pi^+$ events in the signal region, (b) the $D^+ \rightarrow K^- \pi^+ \pi^+$ events in the background region, and (c) the $D^+ \rightarrow K^- \pi^+ \pi^+$ simulated background.

For instance, in the $D^+ \rightarrow K^- \pi^+ \pi^+$ mode the resolution in the two-body invariant mass is $5 \text{ MeV}/c^2$ and after correction reduces to $2 \text{ MeV}/c^2$, which is small compared to the width of a resonance such as the $K^*(892)$. For the $D^0 \rightarrow K^- \pi^+ \pi^0$ mode we used the additional constraint of the π^0 mass and modified the energies and positions of the π^0 decay photons since these are the kinematic variables which dominate the smearing in this case. The fraction of background under the signal (b) is determined from the number of events in the wings of the peak in the mass plot. The background is parametrized free of any specific functional form by subdividing the allowed Dalitz-plot kinematic region iteratively into smaller squares until the number of events in each square is too small or the area of the square is sufficiently small (adaptive binning). In this way we can accurately reproduce the background distribution in a model-independent way for both high- and low-statistics samples. The background is then simulated by a Monte Carlo program for fitting purposes using this parametrization. The simulated background for the $D^+ \rightarrow K^- \pi^+ \pi^+$ mode is shown in Fig. 2. The acceptance over the Dalitz plot is determined from a Monte Carlo simulation. The rms variation was found to be 10% of the mean for the $D^+ \rightarrow K^- \pi^+ \pi^+$ mode, 45% of the mean in the $D^0 \rightarrow K^- \pi^+ \pi^0$ mode, and 95% of the mean in the $D^0 \rightarrow \bar{K}^0 \pi^+ \pi^-$ mode. We parametrized the acceptance in two different ways: as a simple bilinear function of the two Dalitz-plot variables and using the adaptive binning scheme described above for the background. In Fig. 3 we show the signal region Dalitz plots for the D^0 modes (note that the signal/background ratio in these modes is much better than in the D^+ case for our choice of cuts).

The two variables chosen to define the axes of the Dalitz plot are the squares of the invariant masses of the two $K\pi$ combinations. If these are denoted as x and y , the signal is assumed to be distributed as a uniform non-resonant term plus a sum over all resonances:

$$S(x,y) = \left| 1 + \sum_{k=1}^n c_k \exp(i\theta_k) F_k^{\text{BW}}(x,y) D_k^{\text{ang}}(x,y) \right|^2,$$

where F_k^{BW} is a normalized Breit-Wigner function and D_k^{ang} describes the angular distribution for the k th resonance. Since we fit only the shape and since there is always one arbitrary phase, the function has the non-resonant amplitude fixed at 1 and the nonresonant phase fixed at 0. We fitted the data to the form $bB(x,y) + (1-b)S(x,y)$, where B is the background function described above and b is the fraction of background events as determined from the $K\pi\pi$ mass spectrum.

In the D^+ case, the resonances tried were the $K^{*0}(892)$, $K^{*0}(1410)$, $K_0^{*0}(1430)$, $K_2^{*0}(1430)$, $K^{*0}(1680)$, $K_3^{*0}(1780)$, and $K_4^{*0}(2045)$. In the $D^0 \rightarrow K^- \pi^+ \pi^0$ mode we tried to fit for the $K^{*0}(892)$, $K^{*-}(892)$, $\rho^+(770)$, $K^{*0}(1410)$, $K^{*-}(1410)$, $K_0^{*0}(1430)$, $K_0^{*-}(1430)$, $K_2^{*0}(1430)$, $K_2^{*-}(1430)$, $K^{*0}(1680)$, $K^{*-}(1680)$, $K_3^{*0}(1780)$, $K_3^{*-}(1780)$, $K_4^{*0}(2045)$, $K_4^{*-}(2045)$, and $\rho_3^+(1690)$. In the $D^0 \rightarrow \bar{K}^0 \pi^+ \pi^-$ mode we tried to fit for the $K^{*-}(892)$, $\rho^0(770)$, $K^{*-}(1410)$,

$K_0^{*-}(1430)$, $K_2^{*-}(1430)$, $K^{*-}(1680)$, $K_3^{*-}(1780)$, $K_4^{*-}(2045)$, $\omega(783)$, $f_0(975)$, $f_2(1270)$, $f_0(1400)$, and $\rho_3(1690)$. We obtained the best values of the parameters c_k and θ_k by the maximum-likelihood method in a simultaneous fit to all resonances listed above and the non-resonant contribution and background. Resonances whose fit fraction fell below 2% or was less than a three standard deviation effect were dropped from the final fit. The projections onto the two or three possible axes and the results of the fit described above are shown in Fig. 4 for the three different modes.

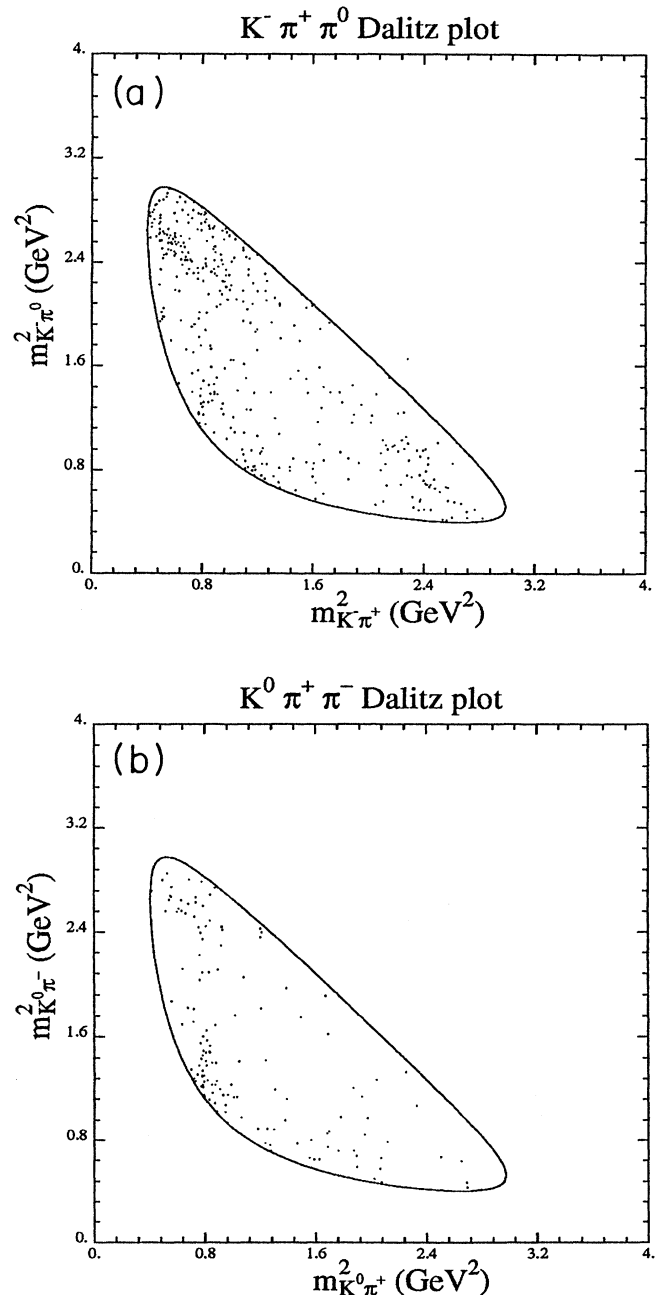


FIG. 3. Dalitz plots for (a) $D^0 \rightarrow K^- \pi^+ \pi^0$ events in the signal region and (b) $D^0 \rightarrow \bar{K}^0 \pi^+ \pi^-$ events in the signal region.

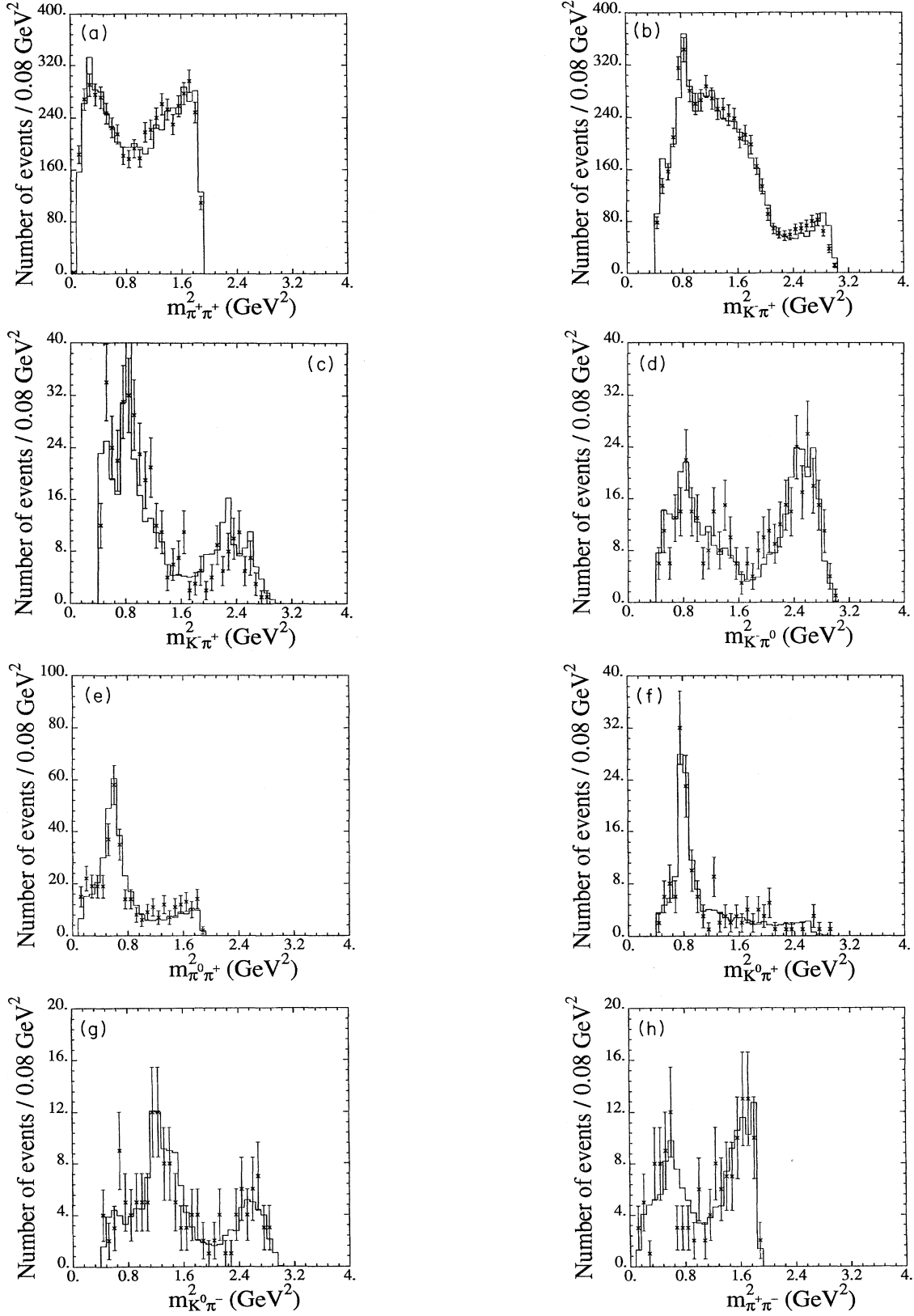


FIG. 4. Projections of the Dalitz plots onto the three axes for the $D^+ \rightarrow K^- \pi^+ \pi^+$ mode [(a) and (b)], the $D^0 \rightarrow K^- \pi^+ \pi^0$ mode [(c), (d), and (e)], and the $D^0 \rightarrow \bar{K}^0 \pi^+ \pi^-$ mode [(f), (g), and (h)]. The points represent the data; the solid line is a projection of the fitted density.

TABLE I. Relative amplitudes and phases from the fits to the Dalitz plot for the $D^+ \rightarrow K^- \pi^+ \pi^+$ mode.

Resonance	Amplitude (c_k)	Phase (θ_k) (deg)	Fit fraction	Branching ratio (%)
Nonresonant $K^- \pi^+ \pi^+$	1	0	0.838	$6.7 \pm 0.7 \pm 2.2$
$\bar{K}^*(892)^0 \pi^+$	0.78 ± 0.02	-60 ± 3	0.170 ± 0.009	$2.0 \pm 0.2 \pm 0.4$
$\bar{K}_0^*(1430)^0 \pi^+$	0.53 ± 0.2	132 ± 2	0.248 ± 0.019	$3.0 \pm 0.4 \pm 0.2$
$\bar{K}^*(1680)^0 \pi^+$	0.47 ± 0.03	-51 ± 4	0.030 ± 0.004	$0.9 \pm 0.2 \pm 0.4$

TABLE II. Relative amplitudes and phases from the fits to the Dalitz plot for the $D^0 \rightarrow K^- \pi^+ \pi^0$ mode.

Resonance	Amplitude (c_k)	Phase (θ_k) (deg)	Fit fraction	Branching ratio (%)
Nonresonant $K^- \pi^+ \pi^0$	1	0	0.036	$0.41 \pm 0.04 \pm 0.2$
$\bar{K}^*(892)^0 \pi^0$	3.19 ± 0.20	167 ± 9	0.142 ± 0.018	$2.4 \pm 0.4 \pm 0.4$
$K^*(892)^- \pi^+$	2.96 ± 0.19	-112 ± 9	0.084 ± 0.011	$2.8 \pm 0.5 \pm 0.4$
$K^- \rho(770)^+$	8.56 ± 0.26	40 ± 7	0.647 ± 0.039	$7.3 \pm 0.8 \pm 1.7$

TABLE III. Relative amplitudes and phases from the fits to the Dalitz plot for the $D^0 \rightarrow \bar{K}^0 \pi^+ \pi^-$ mode.

Resonance	Amplitude (c_k)	Phase (θ_k) (deg)	Fit fraction	Branching ratio (%)
Nonresonant $\bar{K}^0 \pi^+ \pi^-$	1	0	0.263	$1.4 \pm 0.13 \pm 0.22$
$K^*(892)^- \pi^+$	2.31 ± 0.23	109 ± 9	0.480 ± 0.097	$3.9 \pm 0.9 \pm 1.0$
$\bar{K}_0^0 \rho(770)^0$	1.59 ± 0.19	-123 ± 12	0.215 ± 0.051	$1.2 \pm 0.3 \pm 0.2$

TABLE IV. Comparison to Mark III results [6] and the BSW [1] and Lee [9] models.

Decay mode	E691 BR (%)	Mark III BR (%)	BSW prediction (%)	Lee prediction (%)
$K^- \pi^+ \pi^+$ final state				
$D^+ \rightarrow (K^- \pi^+ \pi^+)_{\text{NR}}$	$6.7 \pm 0.7 \pm 2.2$	$7.2 \pm 0.6 \pm 1.8$		
$D^+ \rightarrow \bar{K}^*(892)^0 \pi^+$	$2.0 \pm 0.2 \pm 0.4$	$1.8 \pm 0.2 \pm 1.0$	0.3	2.4
$D^+ \rightarrow \bar{K}^0 \pi^+ \pi^0$ final state				
$D^+ \rightarrow \bar{K}_0^*(1430)^0 \pi^+$	$3.0 \pm 0.4 \pm 0.2$			
$D^+ \rightarrow \bar{K}^*(1680)^0 \pi^+$	$0.9 \pm 0.2 \pm 0.4$			
$K^- \pi^+ \pi^0$ final state				
$D^0 \rightarrow (K^- \pi^+ \pi^0)_{\text{NR}}$	$0.41 \pm 0.04 \pm 0.18$	$1.2 \pm 0.2 \pm 0.6$		
$D^0 \rightarrow \bar{K}^*(892)^0 \pi^0$	$2.4 \pm 0.4 \pm 0.4$	$2.6 \pm 0.3 \pm 0.7$	1.4–3.9	0.73
$D^0 \rightarrow K^*(892)^- \pi^+$	$2.8 \pm 0.5 \pm 0.4$	$4.9 \pm 0.7 \pm 1.5$	3.7–9.1	4.9
$D^0 \rightarrow K^- \rho^+$	$7.3 \pm 0.8 \pm 1.7$	$10.8 \pm 0.4 \pm 1.7$	12.5–13.8	8.7
$\bar{K}^0 \pi^+ \pi^-$ final state				
$D^0 \rightarrow (\bar{K}^0 \pi^+ \pi^-)_{\text{NR}}$	$1.4 \pm 0.13 \pm 0.22$	$2.1 \pm 0.3 \pm 0.7$		
$D^0 \rightarrow K^*(892)^- \pi^+$	$3.9 \pm 0.9 \pm 1.0$	$5.3 \pm 0.4 \pm 1.0$	3.7–9.1	4.9
$D^0 \rightarrow \bar{K}_0^0 \rho(770)^0$	$1.2 \pm 0.3 \pm 0.2$	$0.8 \pm 0.1 \pm 0.5$	0.9–1.1	0.38

IV. RESULTS

The results are summarized in Tables I, II, and III and include the contributions of all resonances which contribute a signal of at least three standard deviations. The fit fraction is determined by integrating each resonance individually over the area of the Dalitz plot and dividing by the integral of $S(x, y)$. The branching ratio is determined by multiplying the fit fraction by the Particle Data Group (PDG) [5] value for the branching ratio in the three-body final state and dividing by the relevant branching ratio of the resonance. The statistical errors on the branching ratios listed in the last column include the error on the fit fraction and the error on the branching ratio for the mode as reported by the PDG [5].

Systematic errors are quoted on the branching ratios and are a quadratic sum of the errors from three possible sources. First, the change observed by dropping resonances from the fit which contributed little to the fit fraction is an estimate of the stability of the fitting procedure. Next, we estimate the accuracy of the Monte Carlo simulation. This is particularly important for the modes involving a π^0 or a K_S^0 . As the second systematic error we consider the change in results after removing, from both data and the Monte Carlo simulation, events with a π^0 below 12 GeV or a K_S^0 below 10 GeV (roughly 10% of our data). Finally, we consider the difference in results using the two different procedures for acceptance corrections described above as the third systematic error. The first two errors described are by far the largest sources of uncertainty, the third being always 1% or less of the corresponding branching ratio.

Among other sources of systematic error considered but judged to be too small is any residual error after smearing is corrected for, event by event. The effect of the Čerenkov-counter-based particle identification is only important for charged kaons since the *a priori* likelihood for a π meson is almost 85%. In the case of kaons the average efficiency is high, around 75% and variations therein are accounted for by the acceptance correction. Last, we implemented relativistic Breit-Wigner amplitudes with an energy-dependent shape [7], but did not find any appreciable difference in the results.

V. CONCLUSION

In conclusion, we find that in the $D^+ \rightarrow K^- \pi^+ \pi^+$ decay the major contribution to the signal is from the non-resonant mode, while for the D^0 decays the resonances

dominate, in particular the $K^*(892)$ and the $\rho(770)$. Our results are consistent with previous measurements [6] by the Mark III Collaboration listed in Table IV. We allowed for more resonances in the fit to the $D^+ \rightarrow K^- \pi^+ \pi^+$ decays than were used by Mark III [6] (see also another analysis of Mark III data [8]). Still, it is clear that the nonresonant mode dominates this channel, making it unique among the $D \rightarrow K \pi \pi$ decays. We note that the $D^0 \rightarrow K^* \pi^+$ branching ratios measured in the two different final states (see Table IV) are consistent with each other and that the branching ratio for $D^+ \rightarrow \bar{K}^*(1680)^0 \pi^+$ is not inconsistent with our results in four-body decay models [4]. Combining the two results yields a branching ratio of $3.02 \pm 0.53\%$. This result can be combined with the decay rates for the modes $D^+ \rightarrow \bar{K}^{*0} \pi^+$ and $D^0 \rightarrow \bar{K}^{*0} \pi^0$ to yield the isospin amplitudes in $D \rightarrow K^* \pi$ decays and their phase difference. We measure $|A_{1/2}| = (3.50 \pm 0.26) \times 10^5 / \sqrt{s}$, $|A_{3/2}| = (0.79 \pm 0.09) \times 10^5 / \sqrt{s}$, $|A_{1/2} / A_{3/2}| = (4.46 \pm 0.64)$, and $(\delta_{1/2} - \delta_{3/2}) = (64^\circ \pm 22^\circ)$. The ratio of amplitudes and the phase difference agree with the values obtained by Mark III [6]. It is interesting that our measurements are also in good agreement with the values measured for $D \rightarrow K \pi$ decays [6].

We also compare our results with predictions from the effective Lagrangian model of Bauer, Stech, and Wirbel [1] (BSW) and the $1/N_C$ model of Lee [9]. These predictions agree well with our measurements within errors. As has been emphasized by many authors, final-state interactions can alter predictions in individual decay modes. Therefore it is better to examine predictions for several final states to look for broad agreement between models and predictions, as we have done here.

ACKNOWLEDGMENTS

We would like to acknowledge useful discussion with E. L. Berger, I. I. Bigi, and B. Stech. We gratefully acknowledge the assistance of the staff of Fermilab and of all the participating institutions. This research was supported by the U.S. Department of Energy, the National Science Foundation, the Natural Science and Engineering Research Council of Canada through the Institute of Particle Physics, the National Research Council of Canada, and the Brazilian Conselho Nacional de Desenvolvimento Científico e Tecnológico. Fermilab is operated by the Universities Research Association, Inc. under contract with the United States Department of Energy.

-
- [1] M. Bauer, B. Stech, and M. Wirbel, *Z. Phys. C* **34**, 103 (1987).
 [2] A. N. Kamal, *Phys. Rev. D* **33**, 1344 (1986).
 [3] J. R. Raab *et al.*, *Phys. Rev. D* **37**, 2391 (1988), and additional references therein.
 [4] J. C. Anjos *et al.*, *Phys. Rev. D* **46**, 1941 (1992).
 [5] Particle Data Group, K. Hikasa *et al.*, *Phys. Rev. D* **45**, S1 (1992).

- [6] J. Alder *et al.*, *Phys. Lett. B* **196**, 107 (1987).
 [7] M. L. Perl, *High Energy Hadron Physics* (Wiley, New York, 1974).
 [8] M. Diakonou and F. Diakonou, *Phys. Lett. B* **216**, 436 (1989).
 [9] D. Lee (private communication); *Phys. Lett. B* **275**, 469 (1992); **277**, 529(E) (1992), describes his model for $D \rightarrow P + P$ decays.